DOI: 10.1002/adem.200800111

EBSD Study on Deformation Twinning in AZ31 Magnesium Alloy During Quasi-in-Situ Compression**

By *Huajie Yang*, *Shuming Yin*, *Chongxiang Huang*, *Zhefeng Zhang*, *Shiding Wu*,* *Shuxin Li*, and *Yandong Liu*

Magnesium alloys are attractive materials due to their excellent mechanical properties such as high specific strength and stiffness, which make them potential candidates for structural components in automotive and aerospace industries.[1] However their poor ability of cold-forming restricts their structural application. The reason is that hexagonal close packed (HCP) metals do not possess five independent equivalent slip systems at room temperature which are required for arbitrary plastic deformation of polycrystals according to the von Mises criterion.[2] On the other hand, mechanical twinning plays an important role in the plastic deformation of magnesium alloys.[3] For metals with a c/a ratio (where a and c are the lattice constants in hexagonal lattices) of less than $\sqrt{3}$ (e.g. magnesium), normally only the $\{10\bar{1}2\}\langle 10\bar{1}1\rangle$ twin is activated by c-axis extension.

The deformation twinning has been widely studied in magnesium and its alloys.[4–11] The factors, including initial texture, grain size, strain path and temperature, have great influence on the twinning behavior. For example, during compression, the grains are favorably oriented if their c-axes are perpendicular to the compression direction and the twinning reorients the c-axes of the twins nearly parallel to the compression direction.[5,12–15] Deformation twinning often has priority to be operated in large grains than in small grains and is easier to occur at lower temperature.[16] Recently some studies focus on the influence of deformation twinning on texture and microstructure evolution.[17,18] Brown et al.[7]used an in-situ neutron diffraction technique to reveal the texture evolution induced by deformation twinning in magnesium, but they did not carry out a systematic evaluation of microstructure evolution during plastic deformation. Jiang et al.[17] chose different strain paths and different temperatures to study the deformation twinning behaviors, they clarified that the initial texture plays a significant role in this process. Later, they further studied the evolution of $\{10\bar{1}2\}\langle 10\bar{1}1\rangle$ twinning during uniaxial compression tests, and found that certain twinning events coincided with specific stages of the flow curve.[19] However, the influence of grain size on $\{10\bar{1}2\}\langle 10\bar{1}1\rangle$ twinning behaviors and the quantitative understanding of the texture and microstructure evolution correlated directly to the amount of deformation twins are relatively rare. In this paper, electron back-scatter diffraction (EBSD) technique was used to study the evolution of texture and microstructure during deformation twinning process of AZ31 magnesium alloy under quasi-in-situ compression to several strain levels along two different directions. The aims of the current study are to analyze the influence of initial texture, grain size and plastic strain on deformation twinning behavior.

Experimental

A commercially hot-extruded AZ31 (Mg-3 %Al-1 %Zn) alloy bar with 18 mm in diameter was used in this study. Two kinds of specimens with dimensions of $4 \times 3 \times 3$ mm^3 were designed to perform the quasi-in-situ compression tests, as shown in Figure 1(a). The sample with compression axis (CA) parallel to the extrusion direction (ED) is denoted as Specimen I; the other with its CA perpendicular to ED is denoted as Specimen II. The EBSD detecting planes for Specimens I and II are also illustrated in Figure 1(a). Before compression tests, the specimens were carefully ground to 3000 grade SiC, then electropolished using the AC-2 electrolyte (Struers, Denmark) at 20 V and at room temperature. The compression tests were carried out at room temperature using a specifically designed specimen holder, which can be

[*] *Dr. H. J. Yang, Prof. S. M. Yin, Prof. C. X. Huang, Prof. Z. F. Zhang, Prof. S. D. Wu, Prof. S. X. Li*
Shenyang National Laboratory for Materials Science
Institute of Metal Research
Chinese Academy of Sciences
72 Wenhua Rd, Shenyang 110016, China
E-mail: shdwu@imr.ac.cn
Dr. S. M. Yin
Shenyang Institute of Chemical Technology
Shenyang, 110142, China
Prof. Y. D. Liu
Northeastern Univ
Sch Mat & Met
Shenyang 110004, China

[**] *The authors thank Ms. W. Gao. for her assistance in the SEM and EBSD experiments, and Dr. W. Z. Han and Dr. F. Yang, for the valuable discussions. This work was financially supported by National Natural Science Foundation of China (NSFC) under grant Nos. 50471082, 50371090 and 50571102. Z. F. Zhang would like to acknowledge the financial support by the National Outstanding Young Scientist Foundation under grant No. 50625103.*

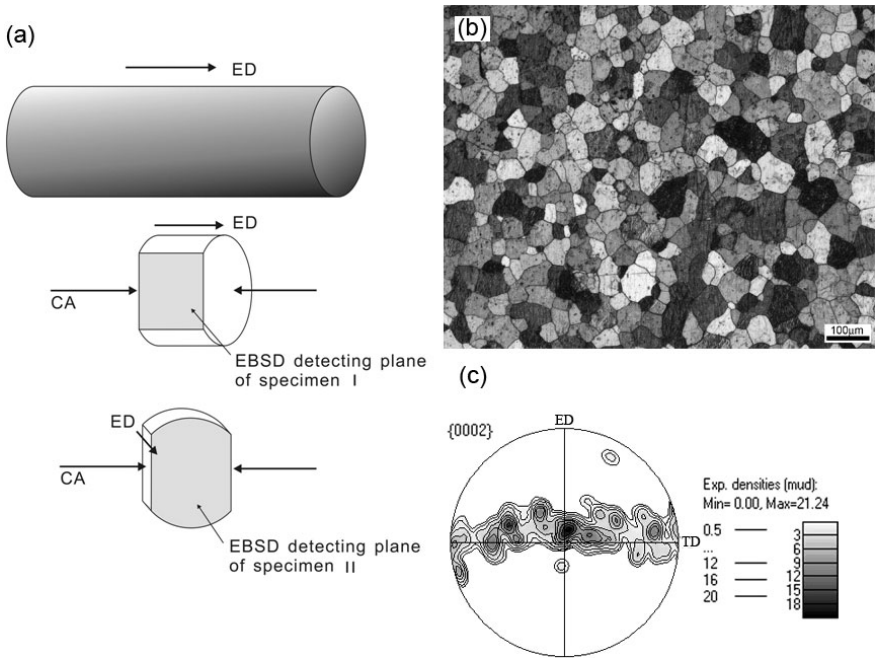

Fig. 1. Schematic of the compression specimens (a): one of which with compression axis (CA) parallel to ED, the other one with CA perpendicular to ED. Optical micrograph (b) and the {0002} pole figure (c) of the as-extruded AZ31 magnesium alloy. The detected plane of (b) is parallel to ED. The EBSD detecting planes of these two kinds of specimens are also indicated in (a).

put into the scanning electron microscope (SEM) chamber together with the specimen under loading. The compression strains were calculated by measuring the two selected positions after each loading. Orientation maps were then collected on the selected area using a LEO Supra 35 field emission SEM equipped with a fully automatic EBSD analysis system (Oxford Instruments-HKL Channel 5). During the EBSD acquisition, a step size of 1.5 μm was chosen. In EBSD orientation maps, we define that the high-angle grain boundary (HAGB) has misorientation larger than 15°, and the low-angle grain boundary (LAGB) has misorientation between 2 ~ 15°, the $\{10\bar{1}2\}$ extension twin boundary (TB) has misorientation of about 86.4 ± 5° $<11\bar{2}0>$. Misorientations less than 2° are neglected. HAGBs, LAGBs and TBs were marked by black, gray and white lines, respectively.

Results and Discussion

Influence of Initial Texture and Plastic Strain on Deformation Twinning

The microstructure and {0002} pole figure (PF) of the initial state are shown in Figure 1(b), 1(c). The grains of the initial material are equiaxed with an average size of ~ 45 μm. A strong {0002} basal plane texture was detected from Figure 1(c). The C-axes of most grains distributed perpendicular to the ED. The EBSD orientation maps of the Specimens I and II under different compression strains are shown in Figure 2.

The initial microstructures of the two specimens (Fig. 3, ε = 0 %) are generally the same: distortion-free grains with sizes from 10 ~ 100 μm, little twin pieces were detected (white lines identified 86 ± 5° TBs). After compressed to a small plastic strain, 4.3 % for Specimen I and 3.3 % for Specimen II, great differences were found. Much more twin pieces were detected in Specimen I than in Specimen II, and the twins in Specimen I are generally thicker than those in Specimen II. These differences indicate that deformation twinning

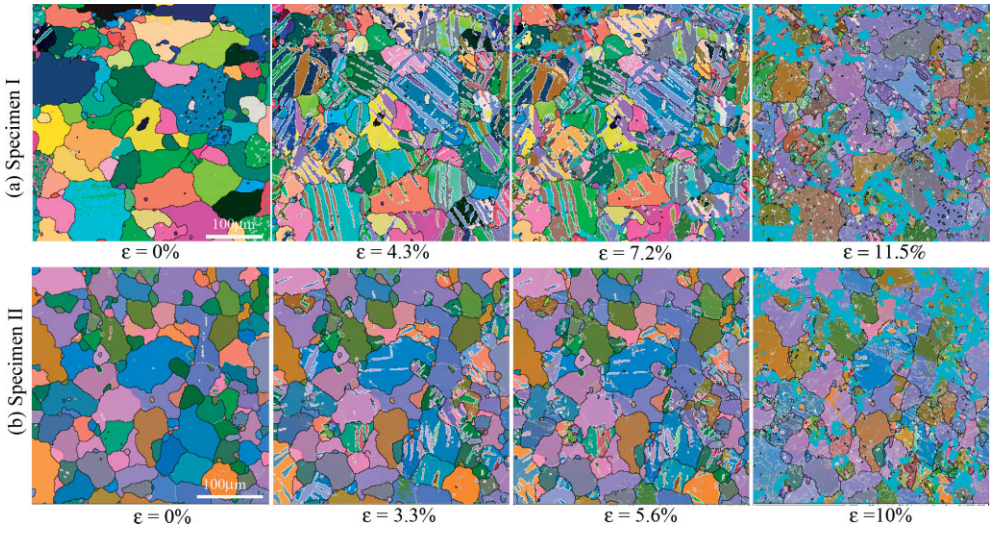

Fig. 2. Euler angle contrast maps of specimen(a): initial, 4.3%, 7.2% and 11.5% compression strains; specimen(b): initial, 3.3%, 5.6% and 10% compression strains. Black lines indicate the HAGBs, white lines indicated the TBs and gray lines indicated the LAGBs. The cyan areas indicate the unindexed areas for the poor surface quality. Compression direction is horizontal. (Color online)

ADVANCED ENGINEERING MATERIALS

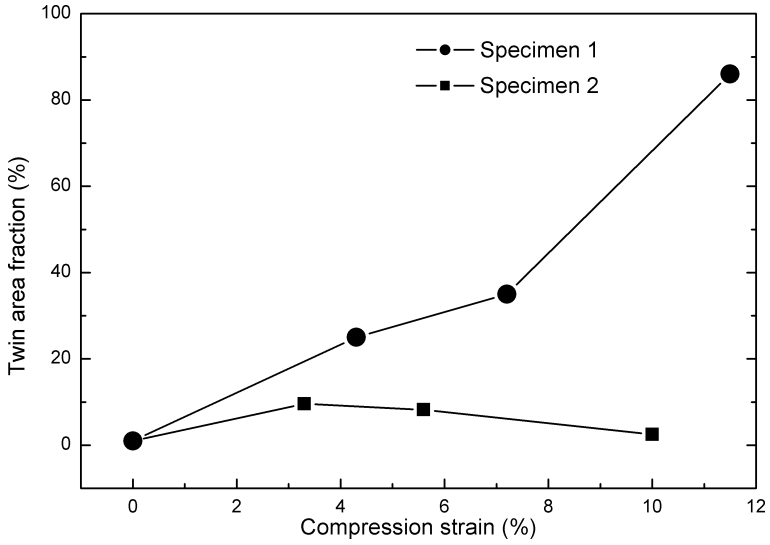

Fig. 3. Twin area fractions of specimen I and specimen II during different compression strains.

is much more easily operated in Specimen I than in Specimen II. Considering that the microstructures of the two specimens are generally the same at the initial state, the reasons may be attributed to the differences in the strain paths and the amount of plastic strains. For Specimen I, its CA is perpendicular to most C-axes of grains, which is a priority direction for $\{10\bar{1}2\}$ tensile twinning in magnesium crystal. However, the CA is parallel to most C-axes of grains in Specimen II, which is a much harder direction for $\{10\bar{1}2\}$ tensile twinning.[19] The initial texture also plays a crucial role in the deformation twinning process, and the influence of texture on deformation twinning will be more significant with the continuous compression process. After the Specimen I was compressed to a strain of 7.2 %, (Fig. 2), the twins have already been widen, leading to the appearance of some new twin segments. After compressed to a strain of 11.5 %, the surface quality of Specimen I became much poorer, the un-indexed area became larger (cyan color areas in the map). In this stage, the TBs did not remain straight and became less; many parent grains were replaced by twins observed from the indexed area, which is similar to the results observed by Jiang et al.[18]. However, the microstructures of the Specimen II compressed to strains of 5.6 % and 10 % showed different characters. The number of twin segments did not increase obviously, and the width of twin bands did not further increase clearly after later compression carried on Specimen II.

The twin area fractions of the Specimens I and II under different strains are shown in Figure 3. For Specimen I, from the initial state to a compression strain of 11.5 %, the twin area fractions are about 1 %, 25 %, 35 % and 86 %, respectively. The twins almost occupied the entire area at last. It means that if grains are favorably oriented, twinning will continue to activate until they are full of the entire area with further loading. For Specimen II, from the initial state to a compression strain of 10 %, the twin area fractions are only about 1 %, 10 %, 8 % and 3 %, respectively. Compared with that of twins in Specimen I, the area fraction of twins in Specimen II is too low when subjected to the same compression strain level, which indicates that it is difficult to be activated for deformation twinning in Specimen II. This result could be attributed to the significant influence of the initial texture (orientation) on deformation twinning in magnesium alloy. Moreover, many LAGBs can be observed from the maps of 11.5 % and 10 % compression strains for Specimens I and II in Figure 2, respectively, indicating that profuse dislocations were multiplied in the two specimens during further loadings.

Influence of Grain Size on Deformation Twinning

To study the effect of grain size on twinning behavior, three grains with different sizes in Specimen I was selected in Figure 4, marked A, B and C with grain size of ~ 100 μm, ~ 40 μm, and ~ 10 μm in diameter, respectively. The initial crystal orientations of these three grains are also shown in the inverse pole figure of Figure 4 (marked with red arrow). From the inverse pole figure, it is clear to find that CA is roughly perpendicular to C-axes of these three grains. So the influence of initial orientation can be neglected. Before compression test, no twin lamella was found in grains A, B and C. After a compression strain of 4.3 %, two different kinds of twin lamellae can be seen in grain A, as marked A-T1 and A-T2 in the map. Although both

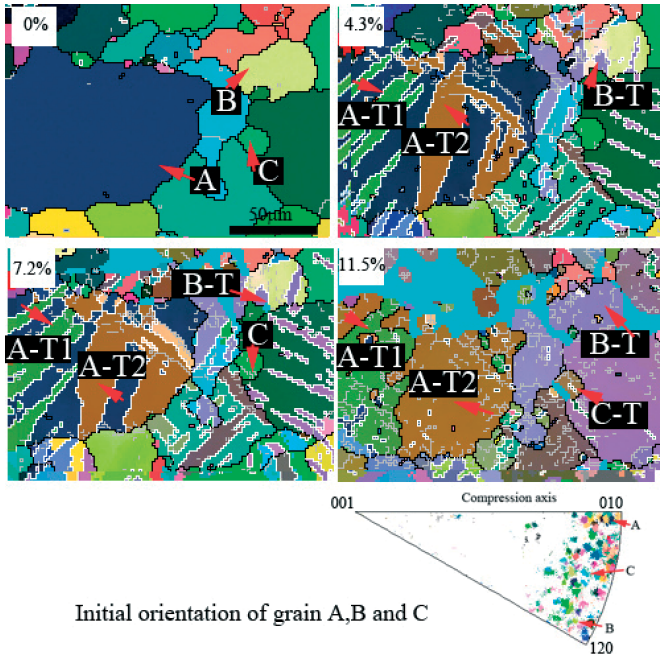

Fig. 4. EBSD orientation maps of grain A, B and C with different sizes in specimen I from initial to 11.5% compression strain, and the initial orientations are also shown in the inverse pole figure. (Color online)

of them belong to {10$\bar{1}$2} extension twins, the orientations are different (color represent orientation). At the same time, just one kind of twin lamella was detected in grain B, and no twin lamella was detected in grain C. In this situation the grain size should be the crucial reason leading to the different deformation twinning behaviors. Meyers et al.[20] have shown that it is common for the twinning stress to increase with decreasing grain size. Barnett et al.[16] also have shown that a transition from twinning to slip dominated flow occurs with decreasing grain size and is accompanied by a lowering of Hall-Petch slope for the yield stress. So in the present study, the grains A, B, and C can be considered as coarse grain, medium grain, and fine grain, respectively. According to Meyers and Barnett's study, it is reasonable that the twinning favorably formed in grain A, existed in grain B, and was restricted in grain C due to the difference in grain sizes. As compression test continued to a strain of 7.5 %, A-T1, A-T2 and B-T became thicker, however, no twin lamella was found in grain C yet. When the compression strain is up to 11.5 %, grain A in the initial state was generally replaced by A-T1 and A-T2, and only a small part of area kept the original orientation. At this time, grain A was split to three grains (A-T1, A-T2 and the initial) by deformation twinning, and grain B was split to two grains (B-T and the initial), however, a small twin lamella was found in grain C finally (marked C-T in the map).

The Texture Evolution of Specimens I and II

The {0002} pole figures (PFs) of Specimens I and II from the initial state to a compression strain of 11.5 % for Specimen I and 10 % for Specimen II are shown in Figure 5(a) and Figure 5(b), respectively. In the initial state, the textures of the two specimens are basically the same. The {0002} PF indicates that almost all C-axes of grains in the two specimens align to perpendicular to ED, and when compression loading is along ED, almost all the grains are favorably oriented for twinning. So, a great amount of twins were nucleated at Specimen I when compressed to a strain of 4.3 %, as shown in Figure 2. When compression strains increase to 4.3 % and 7.2 %, C-axes of the Specimen I gradually rotated to ED, and to a compression strain of 11.5 %, almost all the C-axes rotated to ED, which means the Specimen I has been totally changed to a new texture.

Figure 5(b) shows the PFs of Specimen II from the initial state to a compression strain of 10 %. In comparison with Specimen I, the texture evolution behavior of Specimen II is obviously different. Most C-axes of Specimen II kept the orientation perpendicular to ED all the time while most C-axes of Specimen I rotated about 90°, which is also due to the different twinning behavior. Besides, {10$\bar{1}$2} extension twin has a misorientation of 86.4 ± 5° between the twinned and the parent grain. If {10$\bar{1}$2} extension twinning occurred, the orientation must be rotated by nearly 90°. Thus, for the Specimen I, large amounts of twins changed the texture greatly; however, the texture was nearly reserved, for the Specimen II with few twins.

The Evolution of Misorientation Angle Distributions in Specimens I and II

Figure 6(a) shows the misorientation angle distributions of Specimen I from the initial state to a compression stain of 11.5 %. The curves indicate that in the initial state the majority of GBs are HAGBs. After compression to a strain of 4.3 %, the frequency of TBs with misorientation angles of 86.4° ± 5° greatly increased. And the fraction of TBs in total is 62 %. The fraction of LAGBs with misorientation angles below 15° increased to 18 %. After compression to a strain of 7.2 %, the

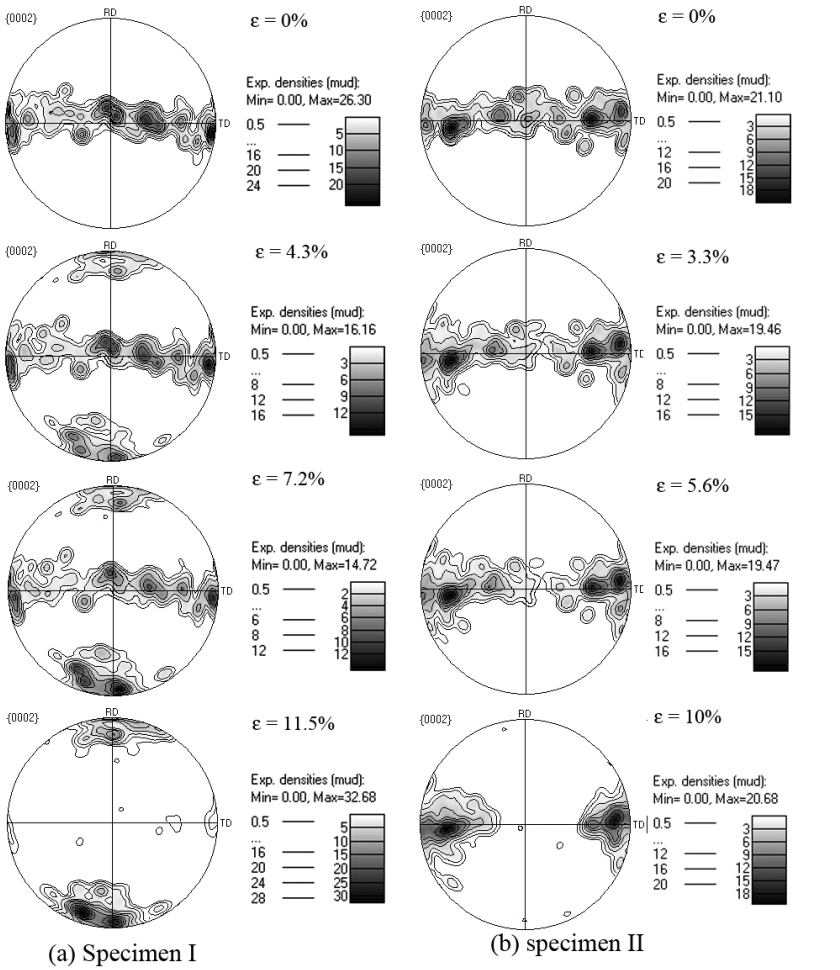

Fig. 5. {0002} *pole figures of specimen I (a) and specimen II (b) after different compression strains.*

fractions of TB and LAGB are 56 % and 23 %, respectively. Notice that the fraction of TB decreased in comparison with that at a compression strain of 4.3 %, the reason is that some TBs are combined together during compression. When the specimen was compressed to a strain of 11.5 %, the TB fraction decreased to 17 % but the LAGB fraction increased to 53 %. LAGB fraction surpasses the TB fraction and becomes the majority part in the misorientation angle distribution. As described before, growth and combination of twin pieces will result in the increase of twin area fraction and the decrease of TB fraction. After a certain compression strain (probably at 10 %), the area fraction of twin approaches to saturation. With the compression process continuing, many dislocations were produced in order to accommodate the further plastic deformation, leading to the increase in LAGB fraction. Figure 6(b) shows the misorientation angle distributions of Specimen II from the initial state to a compression stain of 10 %. Compared to Specimen I, the obvious difference is that the TB fraction is much lower at each strain level, and LAGBs take the majority all the time during deformation. The reasons can be attributed to the different twinning behavior: the same as texture evolution. Since the maximum twin area fraction and the maximum TB fraction for Specimen II were obtained at the strain of 3.3 %, the saturation strain for twinning is probably about 3 %. Because the two different strain paths selected in the present work are on the opposite direction, so the saturate strain for twinning for other strain paths should be in the range of 3 % to 10 %.

Conclusions

Different twinning processes according to the applied compression strains under two kinds of compression directions were found in the present study. For the current quasi-in-situ compression technique, EBSD results clearly show that the strain path is the crucial factor for deformation twinning in magnesium alloys with strong initial basal texture, and the plastic strain and grain size can affect the amount of deformation twins. After $\{10\bar{1}2\}$ extension twinning taking place, the texture would be modified greatly. When loading direction is in favor of $\{10\bar{1}2\}$ extension twinning, there is a saturation stain of about 10 % for twinning; in other loading directions, the saturation stain for twinning is less than 10 %, and further deformation will produce many LAGBs.

Received: April 11, 2008
Final version: June 15, 2008

[1] J. Davis, *Int. Congress and Exposition*. SAE International, **1991**.
[2] V. Mises, R. Agnew, *Math Mech.* **1928**, *8*, 161.
[3] J. T. Wang, D. L. Yin, J. Q. Liu, J. Tao, Y. L. Su, X. Zhao, *Scr. Mater.* **2008**, in press.
[4] M. R. Barnett, in, Icotom 14: *Textures of Mater. Pts 1 and 2*, **2005**, 1079–1084.
[5] L. Jiang, J. J. Jonas, A. A. Luo, A. K. Sachdev, S. Godet, *Scr. Mater.* **2006**, *54*, 771.
[6] Y. N. Wang, J. C. Huang, *Acta Mater.* **2007**, *55*, 897.
[7] D. W. Brown, S. R. Agnew, M. A. M. Bourke, T. M. Holden, S. C. Vogel, C. N. Tome, *Mater. Sci. Eng., A.* **2005**, *399*, 1.
[8] Z. Keshavarz, M. R. Barnett, *Scr. Mater.* **2006**, *55*, 915.
[9] A. Rohatgi, K. S. Vecchio, I. G. T. Gray, *Metall Mater Trans A.* **2006**, *32*, 135.
[10] J. Jiang, A. Godfrey, W. Liu, Q. Liu, *Scr. Mater.* **2008**, *58*, 122.
[11] M. R. Barnett, *Mater. Sci. Eng. A.* **2007**, *464*, 8.
[12] S. R. Agnew, M. H. Yoo, C. N. Tome, *Acta Mater.* **2001**, *49*, 4277.

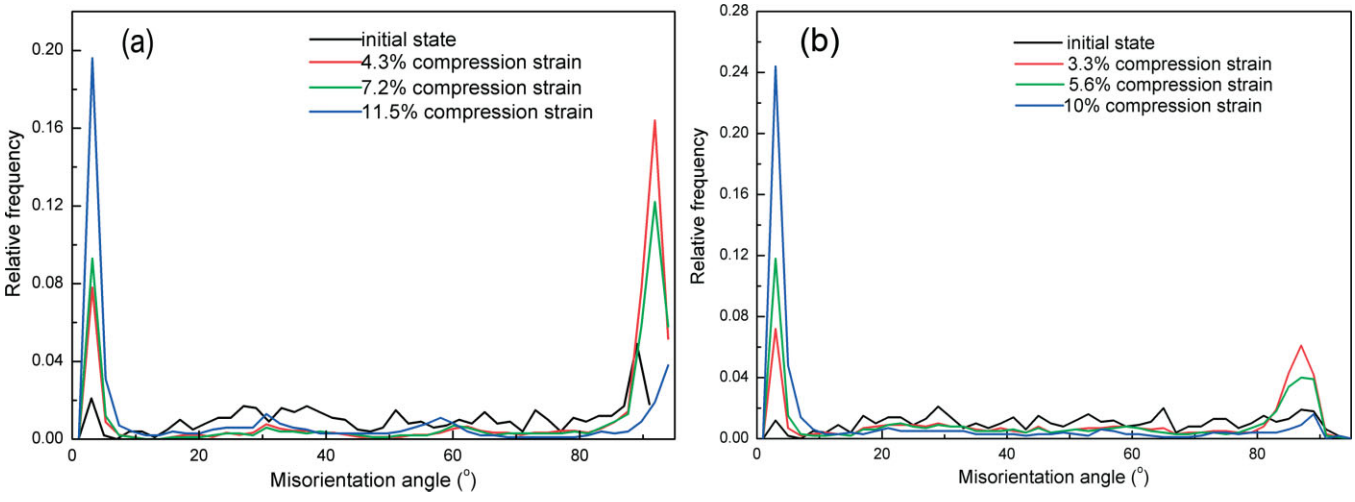

Fig. 6. Misorientation angle distributions of specimen I (a) and specimen II (b) after different compression strains. (Color online)

[13] Q. L. Jin, S. Y. Shim, S. G. Lim, *Scr. Mater.* **2006**, *55*, 843.
[14] P. Yang, Y. Yu, L. Chen, W. Mao, *Scr. Mater.* **2004**, *50* 1163.
[15] S. Godet, L. Jiang, A. A. Luo, J. J. Jonas, *Scr. Mater.* **2006**, *55*, 1055.
[16] M. R. Barnett, Z. Keshavarz, A. G. Beer, D. Atwell, *Acta Mater.* **2004**, *52*, 5093.
[17] L. Jiang, J. J. Jonas, R. K. Mishra, A. A. Luo, A. K. Sachdev, S. Godet, *Acta Mater.* **2007**, *55*, 3899.
[18] J. Jiang, A. Godfrey, W. Liu, Q. Liu, *Mater. Sci. Eng. A.* **2008**, in press.
[19] L. Jiang, J. J. Jonas, A. A. Luo, A. K. Sachdev, S. Godet, *Mater. Sci. Eng. A.* **2007**, *445*, 302.
[20] M. A. Meyers, O. Vohringer, V. A. Lubarda, *Acta Mater.* **2001**, *49*, 4025.

